Geophysical Research Letters

RESEARCH LETTER
10.1029/2018GL077847

# Enhanced Rates of Regional Warming and Ocean Acidification After Termination of Large-Scale Ocean Alkalinization

**Miriam Ferrer González**[1], **Tatiana Ilyina**[1], **Sebastian Sonntag**[1], **and Hauke Schmidt**[1]

[1]Max Planck Institute for Meteorology, Hamburg, Germany

**Key Points:**
- Termination of ocean alkalinization poses higher risks regarding environmental consequences than previously thought
- Regional warming trends after termination of ocean alkalinization resemble those after termination of solar geoengineering
- Ocean acidification rates after termination of ocean alkalinization largely outpace those of the reference RCP8.5 scenario

**Supporting Information:**
- Supporting Information S1

**Correspondence to:**
M. F. González,
miriam.ferrer-gonzalez@mpimet.mpg.de

**Citation:**
González, M. F., Ilyina, T., Sonntag, S., & Schmidt, H. (2018). Enhanced rates of regional warming and ocean acidification after termination of large-scale ocean alkalinization. *Geophysical Research Letters*, *45*, 7120–7129. https://doi.org/10.1029/2018GL077847

Received 8 MAR 2018
Accepted 13 JUN 2018
Accepted article online 21 JUN 2018
Published online 23 JUL 2018

**Abstract** Termination effects of large-scale artificial ocean alkalinization (AOA) have received little attention because AOA was assumed to pose low environmental risk. With the Max Planck Institute Earth system model, we use emission-driven AOA simulations following the Representative Concentration Pathway 8.5 (RCP8.5). We find that after termination of AOA warming trends in regions of the Northern Hemisphere become ~50% higher than those in RCP8.5 with rates similar to those caused by termination of solar geoengineering over the following three decades after cessation (up to 0.15 K/year). Rates of ocean acidification after termination of AOA outpace those in RCP8.5. In warm shallow regions where vulnerable coral reefs are located, decreasing trends in surface pH double (0.01 units/year) and the drop in the carbonate saturation state (Ω) becomes up to 1 order of magnitude larger (0.2 units/year). Thus, termination of AOA poses higher risks to biological systems sensitive to fast-paced environmental changes than previously thought.

**Plain Language Summary** Climate engineering (CE) methods are intended to alleviate the environmental perturbations caused by climate change and ocean acidification. However, these methods can also lead to environmental issues. Among all the different CE techniques, the method of artificial ocean alkalinization (AOA) is commonly discussed. AOA involves the release of processed alkaline minerals into the ocean, which enhances the uptake of atmospheric carbon by the ocean while reducing the acidification of seawater. We study the impacts caused by the termination of AOA on environmental properties that are relevant for organisms and ecosystems because they are sensitive not only to the magnitude of environmental change but also to its pace. We analyze the rate at which the environment changes after termination of this method using an Earth system model that simulates the response of our climate to CE. We found that the abrupt termination of large-scale implementation of AOA leads to regional rates of surface warming and ocean acidification, which largely exceed the pace of change that the implementation of AOA was intended to alleviate. This enhanced rate of environmental change would restrict even more the already limited adaptive capacity of vulnerable organisms and ecosystems.

## 1. Introduction

Various climate engineering (CE) techniques have been proposed to slow down the projected rates of climate change and ocean acidification (e.g., Intergovernmental Panel on Climate Change, 2012; National Research Council, 2015a, 2015b). Artificial ocean alkalinization (AOA) is a carbon dioxide removal method that aims at artificially enhancing the alkalinization of the oceans, which naturally occurs via weathering fluxes over multimillennial time scales (e.g., Hartmann et al., 2013; Kheshgi, 1995). The method of AOA consists of increasing the seawater buffering capacity (Wolf-Gladrow et al., 2007) so that the ocean carbon sink is boosted while seawater pH rises when large amounts of alkalinity are added at the surface. This technique modulates surface temperatures differently than the solar geoengineering method of stratospheric sulfur injection (SSI; e.g., Crutzen, 2006; Niemeier et al., 2013) because the two methods affect different atmospheric forcings: AOA reduces absorption of longwave radiation by lowering $CO_2$ and SSI increases reflectance of solar shortwave radiation.

Termination effects of carbon dioxide removal methods such as AOA have been assumed to pose low to no risk to the environment (e.g., Royal Society, 2009), thereby having received little attention. This is mainly because the temperature response associated with changes in radiation via $CO_2$ involves longer (of the order of decades) time scales than those caused by changes in radiation due to SSI. The termination effects of SSI

are well known, and they pose an ecological threat due to the rapid warming following cessation (e.g., Jones et al., 2013). Still, similar to SSI, whether any future implementation of AOA can be constantly maintained over time or not remains unknown, and hence, potential termination effects of this technique should not be overlooked.

Previous modeling studies have considered terminated AOA scenarios using ocean-only configurations (e.g., Hauck et al., 2016; Ilyina, Wolf-Gladrow, et al., 2013) or Earth system models of intermediate complexity (e.g., Feng et al., 2016; Keller et al., 2014). These studies have not analyzed the short-term (multiyear) response to AOA of environmental properties driving biological processes such as surface atmospheric temperatures and ocean biogeochemistry. Lenton et al. (2018) compared the global and regional responses to AOA over this century by simulating alkalinization scenarios under both high and low emissions pathways. None of the previous comparisons have investigated regional responses of the global carbon cycle to AOA or SSI despite their importance for understanding the Earth system response to anthropogenic perturbations. We gain a broader perspective when comparing the AOA-driven effects of termination to those associated with termination of SSI under the proper modeling framework, which allows us to better evaluate benefits and risks of these methods (e.g., Sonntag et al., 2018).

Here we address the termination-driven impacts of AOA and SSI on surface atmospheric warming, ocean, and land carbon sinks as well as on multiple environmental stressors of ocean ecosystems, namely, changes in temperature, primary production, deoxygenation and acidification (Bopp et al., 2013). Our idealized AOA and SSI simulations are based on the Representative Concentration Pathways (RCPs; van Vuuren et al., 2011, and references therein), and they are forced by the high emissions scenario RCP8.5. We use the Max Planck Institute Earth system model (MPI-ESM) forced by $CO_2$ emissions (i.e., with prognostic treatment of atmospheric $CO_2$ concentration). We study a terminated large-scale AOA scenario and quantitatively compare the rates of environmental change caused by the abrupt termination of AOA to those in the RCP8.5 scenario without CE. Furthermore, using the same modeling framework, we compare the effects of this terminated AOA scenario to those associated with a terminated scenario of SSI. Differently than previous studies, our modeling tool provides an internally consistent representation of CE-driven effects on the carbon cycle because the MPI-ESM includes a comprehensive representation of the interaction between the different elements of the global carbon cycle. We consider comparable AOA and SSI scenarios by defining the intensity of AOA and SSI so that their effects on the Earth system target a similar global mean temperature namely the one of the RCP4.5 scenario. Our focus is on the response of the natural environment to these geoengineering strategies, leaving aside any socioeconomic aspects or technical limitations of these methods.

## 2. Methodology

### 2.1. Model Scenarios of CE

CE scenarios are implemented in the emission-driven MPI-ESM in the low-resolution configuration used in the fifth phase Coupled Model Intercomparison Project (CMIP5; Giorgetta et al., 2013, and references therein). Our simulations of AOA and SSI are compared to the scenarios RCP8.5 and RCP4.5 because they are forced by the $CO_2$ emissions according to RCP8.5, and the intensity of the implementation of CE is defined to achieve a similar climate state by targeting different parameters of the RCP4.5. All experiments are integrated from 2006 to 2100, and the CE methods are either applied until 2100 or terminated in 2070.

In the AOA simulations surface ocean alkalinity is enhanced as much as needed to stabilize atmospheric $CO_2$ concentrations to RCP4.5 levels under RCP8.5 emissions until the end of this century (AOA2100, hereafter) or until the year 2070 (AOA2070). In our purposely idealized experiments, we add alkalinity every time step and spatially homogeneous (i.e., same amount per unit area) into the first ocean model level. This also includes oceanic areas covered by sea ice, such that alkalinity is added in seawater under the ice. Thereby, we follow a generic idealized treatment of the weathering fluxes in the model HAMOCC (HAMburg Ocean Carbon Cycle model) (as described in, e.g., Ilyina, Six, et al., 2013). Such approach allows for a more transparent assessment of the potential environmental consequences of the global large-scale alkalinization.

The AOA2100 and AOA2070 scenarios would require, respectively, additions of around 114 and 45 Pmol of alkalinity. The scale of these perturbations is rather large since, for instance, the provision of 114 Pmol of alkalinity would demand a minimum supply of $\sim 4.22 \cdot 10^{12}$ tons of lime and therefore an enhancement of its production by 2 orders of magnitude until 2100 (see González & Ilyina, 2016, for further details).

The addition of alkalinity in our AOA2070 experiment is large compared with AOA simulations in previous studies: fivefold larger than in Hauck et al. (2016), over half of the integration time, that is, 300 Pg during 100 years versus 1,580 Pg over 50 years assuming olivine as source of alkalinity. In comparison with the addition of alkalinity defined in the Carbon Dioxide Removal Model Intercomparison Project (Keller et al., 2018), we assume a total addition 6 times larger. However, actual availability of raw alkaline materials does not pose the major feasibility issue that AOA faces but rather the associated high logistic costs and environmental problems caused by the mining, production, and release of alkalinity compounds in seawater (e.g., Hartmann et al., 2013; Renforth & Henderson, 2017).

The response of ocean biogeochemistry to CE is simulated by the model HAMOCC, which includes the main biogeochemical processes occurring at the atmosphere-ocean interface, water column, and sediments (Ilyina, Six, et al., 2013). We only consider a terminated AOA scenario, but its effects on surface atmospheric temperatures are equivalent to those associated with a different scenario with a similar trajectory of atmospheric $CO_2$, independent of the means to achieve it (e.g., without AOA but carbon capture and storage). This is because the effects on surface temperatures driven by our simulations of AOA are only induced by the associated changes in atmospheric $CO_2$ levels without additional biogeophysical effects.

The SSI scenarios are defined such that the stratospheric sulfate aerosol distribution reduces the net radiative forcing of the RCP8.5 scenario to RCP4.5 levels until 2100 (SSI2100; as in Sonntag et al., 2018) or only until the year 2070 (SSI2070). The atmospheric component of the MPI-ESM, ECHAM6 does not allow for the interactive simulation of aerosols. Thus, following the approach of Niemeier et al. (2013), the radiative effects of the sulfate aerosols are considered by prescribing their atmospheric optical properties, which were determined using the aerosol microphysical model HAM (Stier et al., 2005) coupled to MAECHAM5 (Giorgetta et al., 2006).

Preliminary simulations were performed in order to diagnose the amount of total alkalinity (TA) to be added and the sulfur injection rate required to meet the goals of the CE scenarios. Model internal variability is considered with an ensemble of three members (differing in their initial conditions) available for each of the simulations.

### 2.2. Regression Analysis for Calculating the Rates of Change

Linear temporal trends are calculated using the Theil-Sen regression technique (Gilbert, 1987), which does not require that the measurement variables are normally distributed. The trends at each grid point are estimated using three ensemble members of each simulation and by fitting the data to $y_t = \alpha + \beta\ t$, where $y_t$ is the annual mean of the variable at year $t$, $\alpha$ is the intercept, and $\beta$ is the nonparametric estimate of the slope. The statistical significance of the linear trends is determined using the Mann-Kendall test that does not require normality (Kendall, 1975; Mann, 1945).

## 3. Results and Discussion

### 3.1. Surface Atmospheric Warming

If carbon emissions continue at the current rate following the RCP8.5 scenario, the MPI-ESM projects that atmospheric $CO_2$ will exceed 950 ppm by the end of this century in line with different models (Figure 1a). This will cause a global warming of around ~3.5 K between the years 2000 and 2100 (Figure 1b). By design of the experiments, the temporal evolution of surface atmospheric temperatures in the AOA2100 and SSI2100 scenarios closely follows the trajectory of the targeted RCP4.5. During the first decade after termination of SSI in 2070 the rates of surface warming largely exceed—up to 1 order of magnitude—those of the RCP8.5 in line with previous estimates (e.g., Jones et al., 2013). Surface atmospheric temperatures rapidly rise in particular over tropical and subtropical regions (Figure 2), in which solar geoengineering in general leads to an overcompensation of global warming (e.g., Schmidt et al., 2012), and hence, its cessation will be felt more strongly than at high latitudes. This strong warming at low latitudes dominates the global trend in the SSI2070 simulation during the first decade following 2070 (Figure 2).

In the AOA2070 scenario, after termination the ocean sink is no longer enhanced leading to a temporal trajectory of atmospheric $CO_2$ that grows parallel to the one of the RCP8.5. $CO_2$ concentrations rise in an atmosphere with lower background $CO_2$ levels than RCP8.5 (Figure 1a) yet at the rate given by RCP8.5 emissions. This leads to a stronger $CO_2$ radiative forcing in the AOA2070 simulation compared to the one of the reference RCP8.5 during the same period of integration, since the $CO_2$ forcing is a logarithmic function of $CO_2$ (Arrhenius, 1896)

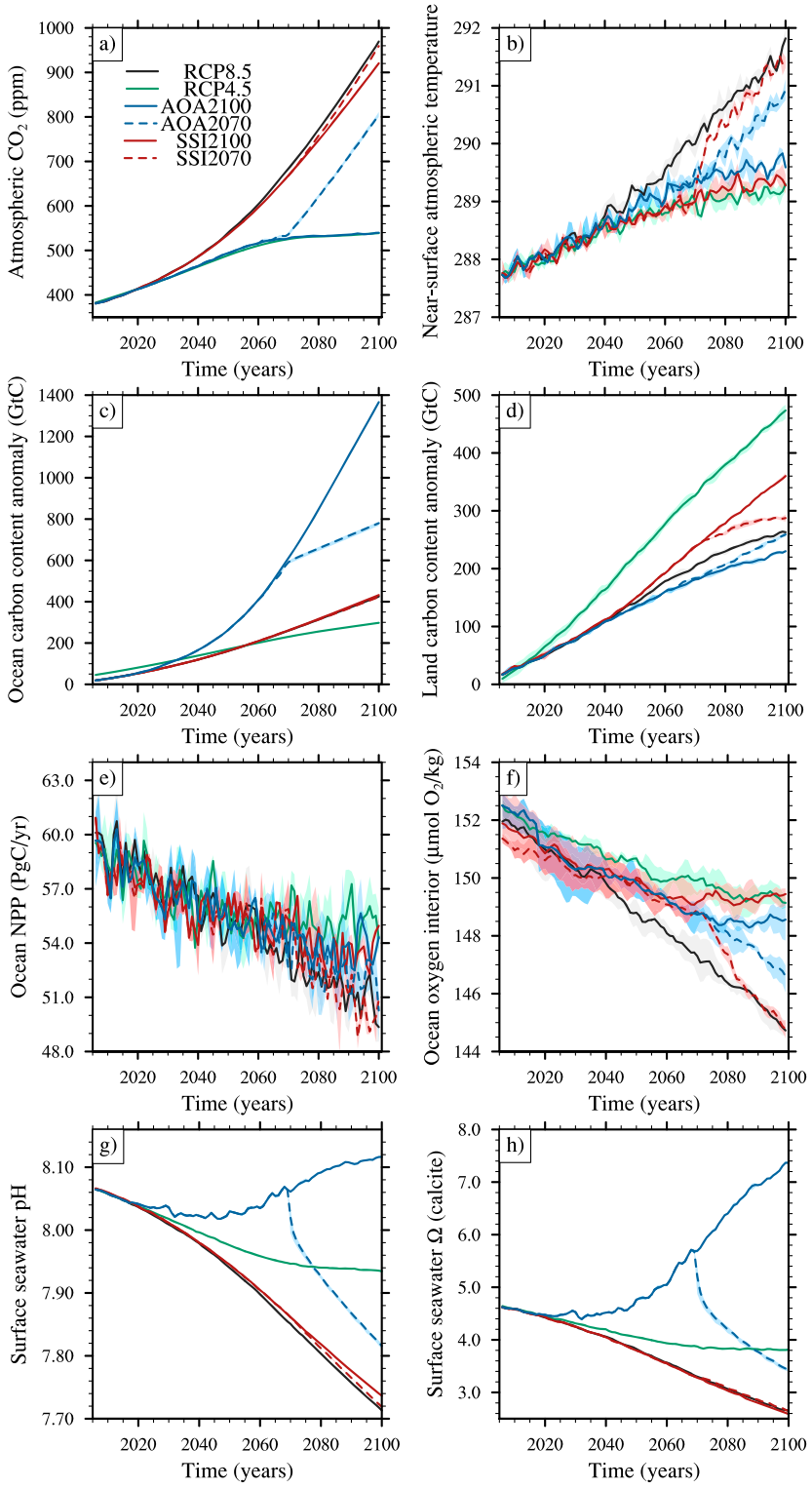


**Figure 1.** Global annual means of (a) atmospheric $CO_2$ (ppm), (b) near-surface atmospheric temperature (K), carbon content anomalies (relative to 2006) in the (c) ocean and the (d) land reservoirs (GtC), (e) ocean net primary production (NPP) globally integrated (PgC/yr), (f) concentration of $O_2$ vertically averaged over 200–600 m (µmol $O_2$/kg), (g) surface seawater pH, and (h) Ω with respect to calcite. Lines depict 5-year running means under the scenarios RCP8.5 (black), RCP4.5 (green), AOA2100 (solid blue), AOA2070 (dashed blue), SSI2100 (solid red), and SSI2070 (dashed red). Colored area is model internal variability including three ensemble members. RCP = Representative Concentration Pathway; AOA = artificial ocean alkalinization; SSI = stratospheric sulfur injection.

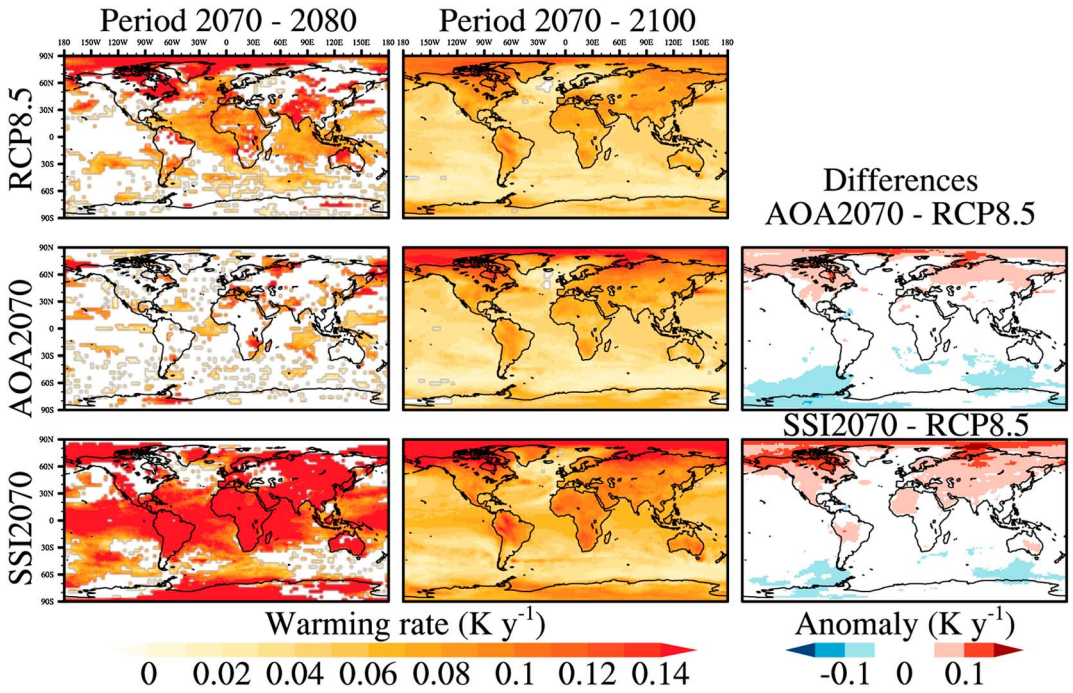


**Figure 2.** Regional trends of near-surface atmospheric temperature (K/year) for the experiments RCP8.5 (first row), AOA2070 (second row), and SSI2070 (third row). First column shows trends during the first decade right after termination of CE (climate engineering from 2070 to 2080). Second column shows trends calculated considering the three decades after termination of CE (from 2070 to 2100) with the differences between these CE experiments and the RCP8.5 (2070–2100) to the right in the third column. Only regions with statistically significant trends at the 95% level are colored. AOA = artificial ocean alkalinization; RCP = Representative Concentration Pathway; SSI = stratospheric sulfur injection.

due to the shape of the $CO_2$ absorption spectrum. For a doubling in atmospheric $CO_2$, the associated radiative forcing ($F_{CO_2}$) may be approximated as (Ramaswamy et al., 2001)

$$F_{CO_2} = 3.7 \cdot \log_2(C/C_0)[\mathrm{W/m^2}],$$

where $C$ is the final concentration of atmospheric $CO_2$ and $C_0$ is the initial level in the time interval over which $CO_2$ changes. Considering the last three decades of integration (i.e., from 2070 to 2100), the $F_{CO_2}$ in the AOA2070 simulation is ~25% higher (0.621 W/m$^2$) than the $F_{CO_2}$ in the RCP8.5 (0.485 W/m$^2$).

Regional rates of atmospheric warming caused by changes in global forcing are uneven, as suggested by measurements and climate change projections (Intergovernmental Panel on Climate Change, 2013). Arctic regions warm faster than the rest of the globe (e.g., Serreze & Barry, 2011), and the greenhouse forcing causes an interhemispheric temperature asymmetry (e.g., Friedman et al., 2013). Differences in forcing and the contrasting temperature response between Earth's hemispheres drive the different regional patterns of surface warming between the AOA2070 and RCP8.5 simulations (Figure 2). In north polar regions and over high latitudes of North America and Europe, considering the last three decades of integration, the warming rates after termination of AOA are nearly 50% higher than the projected rates in RCP8.5 for this period. They reach up to 0.15 K/year, similar to the warming rates associated with the terminated SSI during the decades from 2070 to 2100 (Figure 2), which are lower than the warming rates in the first decade right after termination of SSI, yet considerably higher than those associated with RCP8.5.

Organisms are sensitive to the pace at which their environment changes (e.g., Pörtner et al., 2014). Quintero and Wiens (2013) have estimated that main vertebrate animal groups will need rates of niche evolution 4 orders of magnitude higher than those generally surveyed in order to adapt to the projected rates of climate change in a high $CO_2$ emissions scenario by the end of this century. Thus, any CE-driven acceleration of the regional rates of surface warming might further inhibit the adaptive capacity of these organisms.

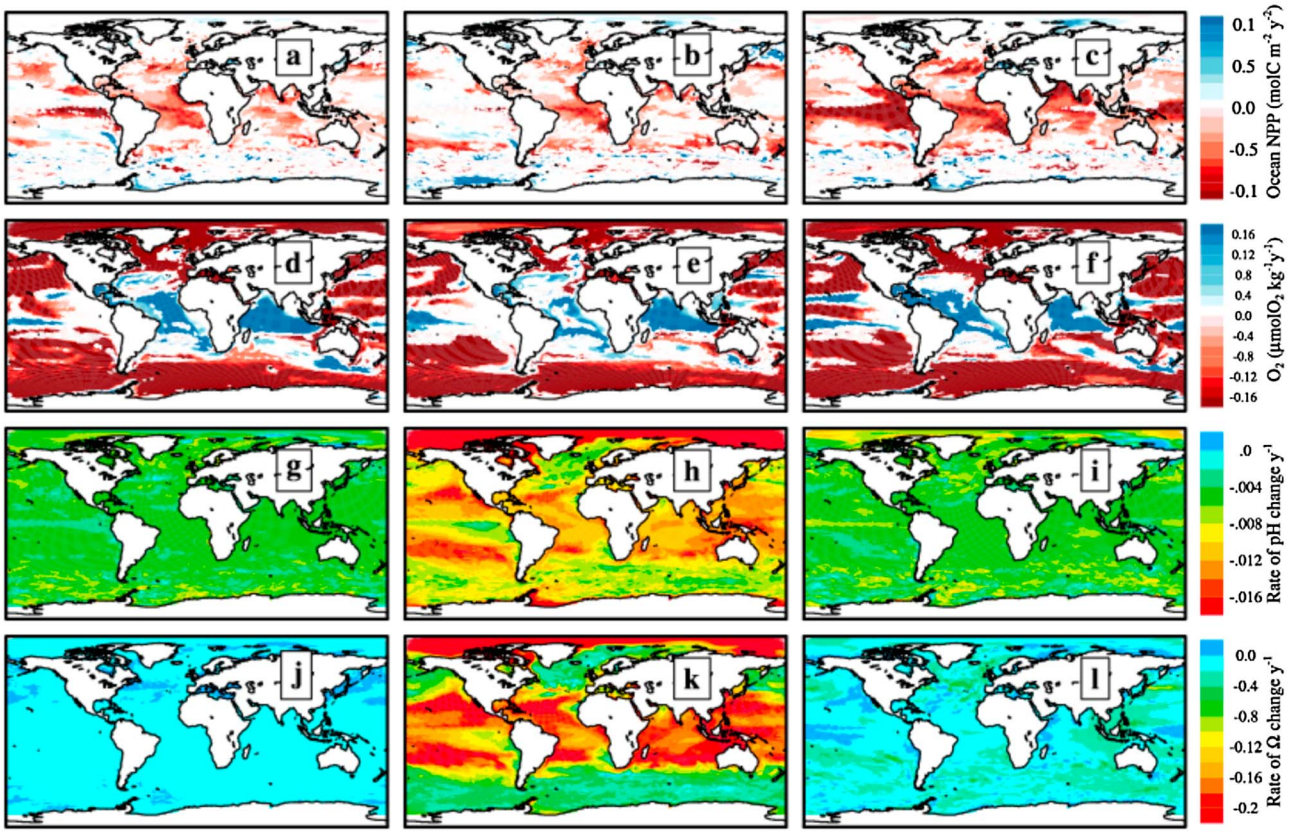


**Figure 3.** Regional trends of ocean net primary production (NPP) vertically integrated (first row), oxygen concentration vertically averaged over the first 200–600 m of the water column (second row), surface seawater pH (third row), and Ω with respect to calcite (fourth row) in the experiments Representative Concentration Pathway 8.5 (first column), AOA2070 (second column), and SSI2070 (third column). In order to enhance the signal to noise ratio, the time interval from 2070 to 2100 is considered for ocean NPP and oxygen at middepths, while for pH and Ω the period from 2070 to 2075 is shown because trends are largest. Only regions with statistically significant trends at the 95% level are colored.

### 3.2. Ocean NPP and Deoxygenation

Under the high emissions scenario RCP8.5, the MPI-ESM projects that global net primary production (NPP) decreases over the course of the 21st century to ~80% of its current value by 2100 (i.e., from 60 to 50 Pg C/yr) (Figure 1e). Regionally, negative trends of NPP emerge in the RCP8.5 over most of the tropical and subtropical oceans (with an average value of −0.05 mol $C \cdot m^{-2} \cdot year^{-2}$) during the last decades of the simulated period (Figure 3a). This is because nutrient supply decreases driven by changes in ocean circulation and mixing, which is characterized by reduced mixed layer depth (Behrenfeld et al., 2006; Bopp et al., 2013).

Regional rates of change in NPP in the AOA2070 simulation are similar to those associated with the reference RCP8.5 from 2070 onward due to their similar regional warming rates over most of the open ocean (Figure 3b). However, in the SSI2070 scenario over tropical and subtropical oceans, there is a doubling of the area in which trends of decreasing NPP become as low as the lowest values reached in the RCP8.5 simulation (approximately −0.05 mol $C \cdot m^{-2} \cdot year^{-2}$; Figure 3c). Moreover, decreasing trends in NPP in the SSI2070 experiment from 2070 onward become up to 1 order of magnitude higher than RCP8.5 over large regions of the tropical oceans due to the rapid adjustment of the mixed layer depth to the accelerated warming right after termination of SSI (supporting information Figure S1).

Similar to the reduction in ocean NPP, deoxygenation poses risks to marine biology (e.g., Bopp et al., 2013; Pörtner et al., 2014). The RCP8.5 shows a general declining trend in oxygen at middepths (within 200–600 m) in large ocean regions over high latitudes (Figure 3d), dominating the global trend, which drops by ~4% relative to current values by 2,100 (Figure 1f). Yet large regions of the Atlantic and Indian Oceans within tropical latitudes show an increasing trend in oxygen content likely caused by changes in remineralization (Bopp et al., 2013). The scenario AOA2070 shows similar trends to those of the RCP8.5 (Figure 3e),

while in the SSI2070 simulation, ocean deoxygenation occurs at a larger rate than in the reference RCP8.5 (Figures 1f and 3f). Specifically, during the first decade after the termination of SSI (from 2070 to 2080), the trend in deoxygenation doubles the pace of the reference scenario RCP8.5.

Internal model variability of oxygen at middepths is relatively large, still, trends are significantly different between the simulations (Figure 1f). Regional trends of oxygen at middepths behave in accordance with the rate of change at which the physical environment varies, with a magnitude of change that is mainly governed by the associated rate of surface warming in each of the scenarios (Figures 3d – 3f). Our results reveal that after termination of SSI, marine ecosystems might be exposed to rapid variations in environmental properties governing key biological processes well outside of the range of natural variability, which must be considered in the evaluation of the CE-driven risks.

### 3.3. Ocean Acidification

While the temperature-induced effects of the different SSI scenarios on surface seawater carbonate chemistry are small, our large-scale AOA simulations show that this method might lead to rapid variations in seawater carbonate chemistry, not only during the implementation of AOA but also after its termination. In the first decade after termination in the AOA2070 scenario, the abrupt interruption of AOA causes that surface seawater acidifies much faster than in the reference RCP8.5 (Figures 1g and 1h). Over the Arctic Ocean and tropical oceans right after termination of AOA in 2070, regional rates of decrease in surface pH reach 0.01 units per year, doubling those projected in the RCP8.5 scenario. Rates of decrease in $\Omega$ (up to 0.2 units per year) become up to 1 order of magnitude larger than those associated with the RCP8.5 (Figures 3g – 3l).

The Arctic Ocean and tropical oceans emerge as especially sensitive regions to these rapid variations after termination of AOA because the rate of increase in dissolved inorganic carbon (DIC) exceeds the rate at which the total alkalinity (TA) content varies in these water masses (i.e., $\Delta DIC > \Delta TA$, supporting information Figure S2). $\Delta DIC$ exceeds $\Delta TA$ because the rate of $CO_2$ invasion (i.e., DIC content) is larger than naturally occurring processes affecting the rate of TA change (i.e., $CaCO_3$ dissolution/formation, photosynthesis, and respiration). $\Delta DIC$ exceeds $\Delta TA$ for all ocean regions in AOA2070, but this difference in the DIC and TA rates is largest in the Arctic, followed by the tropics.

In the open ocean, differences in the rates of change between DIC and TA are mainly driven by the pace at which the strong bases are added into the surface seawater during AOA and by the rate at which the carbonate system returns to equilibrium. In shallow oceans where vertical mixing is constrained by thermal stratification, the enhanced uptake of $CO_2$ following AOA may not compensate the disequilibrium in the partitioning of the carbonate species, leading to large regional differences despite the globally homogeneous distribution of TA.

Over the Arctic Ocean, sea ice retreat accentuates this differential rate of variation between DIC and TA because the exposure of alkaline cold water to the atmosphere further enhances the rate of $CO_2$ invasion (i.e., DIC content). This leads to a much faster pace of ocean acidification in the Arctic relative to the rest of the ocean, which is an effect of our scenario design in which TA is also added over areas covered by sea ice (Figure 3h).

Our results show that termination effects of AOA on the carbonate chemistry depend linearly on the amount of added alkalinity. The specific regional rates of variation largely depend upon the background seawater state, but in general, the greater the addition of alkalinity prior termination, the faster the convergence toward the seawater state without the effects of AOA.

A field study suggests that AOA might actually alleviate the observed decrease in the net community calcification of coral reefs in acidified seawater (Albright et al., 2016). However, our results show that the abrupt termination of this method might damage keystone species in the reef ecosystem, which are especially sensitive to a fast-paced acidification of seawater. The coralline algae *Lithothamnion glaciale* exposed to a fast drop in pH suffers structural damages (Kamenos et al., 2013). And yet the same decrease in pH occurring at a slower pace does not cause any harm. Thus, individual keystone species within the coral reefs might be negatively affected by these fast-paced environmental changes after termination of AOA but the response of the entire ecosystem remains unknown. Rapid variations in the environment are generally detrimental for the ecosystem functioning, as observed in aquaculture practices, which require relatively stable conditions in order to ensure high growth and survival rates (e.g., Wurts & Durborow, 1992).

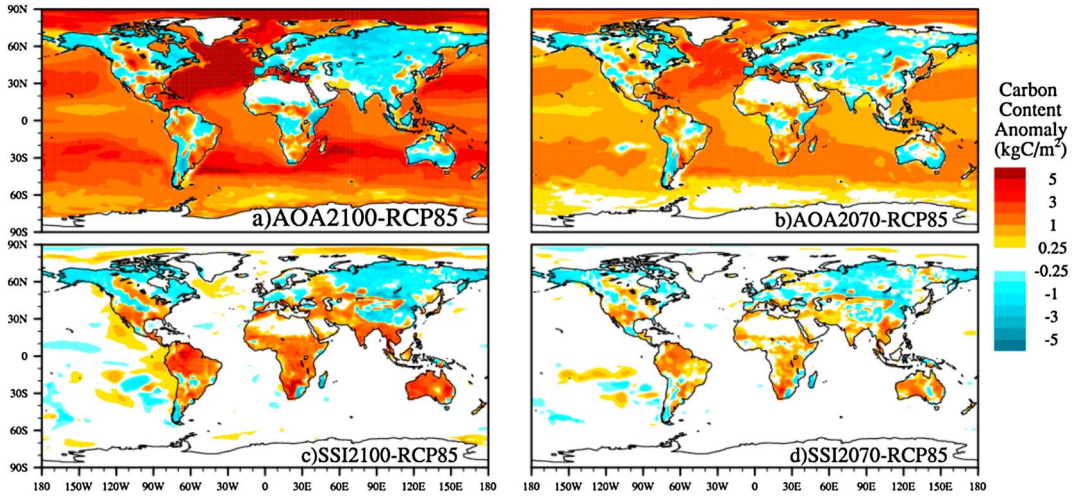


**Figure 4.** Anomalies of the terrestrial and oceanic carbon budgets: differences between the carbon reservoirs of the climate engineering scenarios (a) AOA2100, (b) AOA2070, (c) SSI2100, and (d) SSI2070 and the reference scenario RCP8.5 in the year 2100. Note the nonlinear color bar. SSI = stratospheric sulfur injection; AOA = artificial ocean alkalinization.

The effects of an abrupt termination of AOA might also interfere with reproductive cycles of fish since the rates of pH change have been identified as trigger for key transitions in their life cycles (e.g., Cornish & Smit, 1995; Fiorillo et al., 2013).

### 3.4. Ocean and Land Carbon Sinks

In our large-scale AOA simulations, the North Atlantic Ocean presents the highest regional carbon uptake by 2100 where deep water formation occurs (Figures 4a and 4b). When the large-scale AOA scenario ends in 2070, the seawater buffering capacity rapidly returns to RCP8.5 levels. The global ocean sink continues tempering the growing atmospheric $CO_2$ concentrations thereafter, yet at the same pace as in the reference RCP8.5 scenario (Figure 1c). Global averages of atmospheric $CO_2$ levels and surface temperatures increase parallel to the RCP8.5 trajectory (Figures 1a and 1b), leading to a growing land carbon content over time (Figure 1d). The land carbon content anomaly in the AOA2070 experiment reaches the same level as the one of the RCP8.5 scenario by 2100 (~250 GtC). The spatial patterns of change in land carbon storage are heterogeneous in our AOA scenarios (Figures 4a and 4b), with a predominant reduction in land carbon content across Eurasia mainly driven by a reduction in terrestrial NPP (Sonntag et al., 2018).

In our SSI simulations we find a modest potential for $CO_2$ removal of this method also found in previous studies (e.g., Keller et al., 2014; Sonntag et al., 2018; Tjiputra et al., 2016), which in our case is dominated by the impacts of SSI on the terrestrial carbon sink. By the end of the century the terrestrial carbon pool in the SSI2100 simulation is 92 GtC higher than in RCP8.5 (Figure 1d), which is equivalent to approximately one decade of $CO_2$ emissions from fossil fuels and industry (Le Quéré et al., 2018). In contrast, the ocean carbon reservoir in the SSI2100 simulation is only 8 GtC higher than in the RCP8.5 scenario (Figure 1c). Regionally, SSI-driven changes in the land carbon content show a net increase over land masses of the Southern Hemisphere, while Northern Hemisphere regions show a more heterogeneous spatial pattern (Figure 4c). After termination of SSI in 2070, the surface warming induces that (globally) almost all the additional carbon relative to RCP8.5 stored in land and ocean returns to the atmosphere (Figures 1c and 1d), despite small regional differences (Figures 4d). Thus, any reduction of atmospheric $CO_2$ levels driven by the effects of SSI completely vanishes within the following decades after SSI is stopped.

## 4. Summary and Conclusions

Using the MPI-ESM with emission-driven simulations, we examine the environmental effects that termination scenarios of AOA and SSI have on global means and regional patterns of surface temperatures, multiple stressors of ocean ecosystems, and the ocean and land carbon sinks. We find that the termination of these CE methods after their implementation on a global scale has large potential to significantly exceed the pace of the environmental change that they were intended to alleviate. We project regional warming rates that exceed those of the reference RCP8.5 scenario not only after termination of SSI but also after termination of AOA.

In north polar regions and over high latitudes of North America and Europe, the rates of surface atmospheric warming from 2070 to 2100 are nearly 50% higher in our terminated AOA simulation than in the RCP8.5, and they become as large as in the terminated SSI scenario (up to 0.15 K/year).

SSI-driven effects on ocean carbonate chemistry are minor in contrast to the rapid variations after termination of AOA. Areas of limited vertical mixing show high sensitivity to termination of AOA owing to a nonparallel rate of variation of TA and DIC after termination. Regional trends in surface ocean acidification over the Arctic Ocean and tropical oceans right after termination of AOA in 2070 largely exceed those projected in the RCP8.5. Surface pH trends (0.01 units per year) double those associated with the RCP8.5 and the annual decrease in $\Omega$ (0.2 units per year) becomes up to 1 order of magnitude larger.

We conclude that the abrupt termination of large-scale AOA causes environmental impacts related to regional accelerated warming and ocean acidification, which pose greater risks to biological systems than previously thought. First, termination of AOA leads to associated rates of niche evolution that exceed those generally surveyed among main vertebrate animal groups in the geological records by more than 4 orders of magnitude (Quintero & Wiens, 2013). And second, the rapid response of the seawater carbonate system to changes in alkalinity induces a fast-paced perturbation in the marine chemical environment, which endangers keystone species within vulnerable ecosystems (Kamenos et al., 2013). Thus, in a similar way to solar geoengineering methods, termination of AOA could entail significant environmental risks.

**Acknowledgments**
This work was funded by the German Science Foundation (DFG) within the Priority Program Climate Engineering: Risks, Challenges, Opportunities (SPP 1689). The German Climate Computing Center (DKRZ) made available the computational resources supported by the German Federal Ministry of Education and Research (BMBF). We appreciate the useful suggestions by Marlene Klockmann and the anonymous reviewer on this manuscript. Scripts and primary data required to reproduce our analysis are archived by the Max Planck Institute for Meteorology and they are available by contacting publications@mpimet.mpg.de.

## References

Albright, R., Caldeira, L., Hosfelt, J., Kwiatkowski, L., Maclaren, J. K., Mason, B. M., et al. (2016). Reversal of ocean acidification enhances net coral reef calcification. *Nature*, *531*(7594), 362–365. https://doi.org/10.1038/nature17155

Arrhenius, S. (1896). On the influence of carbonic acid in the air upon the temperature of the ground. *Philosophical Magazine and Journal of Science*, *41*(251), 237–276. https://doi.org/10.1080/14786449608620846

Behrenfeld, M. J., O'Malley, R. T., Siegel, D. A., McClain, C. R., Sarmiento, J. L., Feldman, G. C., et al. (2006). Climate-driven trends in contemporary ocean productivity. *Nature*, *444*(7120), 752–755. https://doi.org/10.1038/nature05317

Bopp, L., Resplandy, L., Orr, J. C., Doney, S. C., Dunne, J. P., Gehlen, M., et al. (2013). Multiple stressors of ocean ecosystems in the 21st century: Projections with CMIP5 models. *Biogeosciences Discussions*, *10*(2), 3627–3676. https://doi.org/10.5194/bgd-10-3627-2013

Cornish, D. A., & Smit, G. L. (1995). The correlation between environmental factors and the reproduction of Oreochromis mossambicus. *Water SA*, *21*, 259–263.

Crutzen, P. J. (2006). Albedo enhancement by stratospheric sulfur injections: A contribution to resolve a policy dilemma? *Climatic Change*, *77*(3), 211. https://doi.org/10.1007/s10584-006-9101-y

Feng, E. Y., Keller, D. P., Koeve, W., & Oschlies, A. (2016). Could artificial ocean alkalinization protect tropical coral ecosystems from ocean acidification? *Environmental Research Letters*, *11*(7), 74008. https://doi.org/10.1088/1748-9326/11/7/074008

Fiorillo, I., Rossi, S., Alva, V., Gili, J. M., & López-González, P. J. (2013). Seasonal cycle of sexual reproduction of the Mediterranean soft coral Alcyonium acaule (Anthozoa, Octocorallia). *Marine Biology*, *160*(3), 719–728. https://doi.org/10.1007/s00227-012-2126-z

Friedman, A. R., Hwang, Y.-T., Chiang, J. C. H., & Frierson, D. M. W. (2013). Interhemispheric temperature asymmetry over the twentieth century and in future projections. *Journal of Climate*, *26*(15), 5419–5433. https://doi.org/10.1175/JCLI-D-12-00525.1

Gilbert, R. O. (1987). *Statistical methods for environmental pollution monitoring*. New York: Van Nostrand Reinhold Co.

Giorgetta, M. A., Jungclaus, J., Reick, C. H., Legutke, S., Bader, J., Böttinger, M., et al. (2013). Climate and carbon cycle changes from 1850 to 2100 in MPI-ESM simulations for the Coupled Model Intercomparison Project Phase 5. *Journal of Advances in Modeling Earth Systems*, *5*, 572–597. https://doi.org/10.1002/jame.20038

Giorgetta, M. A., Manzini, E., Roeckner, E., Esch, M., & Bengtsson, L. (2006). Climatology and forcing of the quasi-biennial oscillation in the MAECHAM5 model. *Journal of Climate*, *19*(16), 3882–3901. https://doi.org/10.1175/JCLI3830.1

González, M. F., & Ilyina, T. (2016). Impacts of artificial ocean alkalinization on the carbon cycle and climate in Earth system simulations. *Geophysical Research Letters*, *43*(12), 6493–6502. https://doi.org/10.1002/2016GL068576

Hartmann, J., West, A. J., Renforth, P., Köhler, P., De La Rocha, C. L., Wolf-Gladrow, D. A., et al. (2013). Enhanced chemical weathering as a geoengineering strategy to reduce atmospheric carbon dioxide, supply nutrients, and mitigate ocean acidification. *Reviews of Geophysics*, *51*, 113–149. https://doi.org/10.1002/rog.20004

Hauck, J., Köhler, P., Wolf-Gladrow, D., & Völker, C. (2016). Iron fertilisation and century-scale effects of open ocean dissolution of olivine in a simulated $CO_2$ removal experiment. *Environmental Research Letters*, *11*(2), 024,007.

Ilyina, T., Six, K. D., Segschneider, J., Maier-Reimer, E., Li, H., & Núñez Riboni, I. (2013). Global ocean biogeochemistry model HAMOCC: Model architecture and performance as component of the MPI-Earth system model in different CMIP5 experimental realizations. *Journal of Advances in Modeling Earth Systems*, *5*, 287–315. https://doi.org/10.1029/2012MS000178

Ilyina, T., Wolf-Gladrow, D., Munhoven, G., & Heinze, C. (2013). Assessing the potential of calcium-based artificial ocean alkalinization to mitigate rising atmospheric $CO_2$ and ocean acidification. *Geophysical Research Letters*, *40*, 1–6. https://doi.org/10.1002/2013GL057981

Intergovernmental Panel on Climate Change (2012). Meeting report of the Intergovernmental Panel on Climate Change expert meeting on geoengineering, Potsdam Institute for Climate Impact Research, Potsdam, Germany. (99 pp.)

Intergovernmental Panel on Climate Change (2013). Climate change 2013: The physical science basis, *Contribution of working group I to the Fifth Assessment Report of the Intergovernmental Panel on Climate Change* (pp. 1535). Cambridge, United Kingdom and New York, NY, USA: Cambridge University Press. https://doi.org/10.1017/CBO9781107415324

Jones, A., Haywood, J. M., Alterskjær, K., Boucher, O., Cole, J. N. S., & Curry, C. L. (2013). The impact of abrupt suspension of solar radiation management (termination effect) in experiment G2 of the Geoengineering Model Intercomparison Project (GeoMIP). *Journal of Geophysical Research: Atmospheres*, *118*, 9743–9752. https://doi.org/10.1002/jgrd.50762

Kamenos, N. A., Burdett, H. L., Aloisio, E., Findlay, H. S., Martin, S., Longbone, C., et al. (2013). Coralline algal structure is more sensitive to rate, rather than the magnitude, of ocean acidification. *Global Change Biology*, *19*(12), 3621–3628. https://doi.org/10.1111/gcb.12351

Keller, D. P., Feng, E. Y., & Oschlies, A. (2014). Potential climate engineering effectiveness and side effects during a high carbon dioxide-emission scenario. *Nature Communications*, *5*, 3304. https://doi.org/10.1038/ncomms4304

Keller, D. P., Lenton, A., Scott, V., Vaughan, N. E., Bauer, N., Ji, D., et al. (2018). The Carbon Dioxide Removal Model Intercomparison Project (CDRMIP): Rationale and experimental protocol for CMIP6, *11*(3), 1133–1160. https://doi.org/10.5194/gmd-11-1133-2018

Kendall, M. (1975). *Rank correlation methods* (4th ed.). London: Charles Griffin.

Kheshgi, H. S. (1995). Sequestering atmospheric carbon dioxide by increasing ocean alkalinity. *Energy*, *20*(9), 915–922. https://doi.org/10.1016/0360-5442(95)00035-F

Le Quéré, C., Andrew, R. M., Friedlingstein, P., Sitch, S., Pongratz, J., Manning, A. C., et al. (2018). Global carbon budget 2017. *Earth System Science Data*, *10*(1), 405–448. https://doi.org/10.5194/essd-10-405-2018

Lenton, A., Matear, R. J., Keller, D. P., Scott, V., & Vaughan, N. E. (2018). Assessing carbon dioxide removal through global and regional ocean alkalinization under high and low emission pathways. *Earth System Dynamics*, *9*(2), 339–357. https://doi.org/10.5194/esd-9-339-2018

Mann, H. B. (1945). Nonparametric tests against trend. *Econometrica*, *13*(3), 245–259. https://doi.org/0012-9682(194507)13:3<245:NTAT>2.0.CO;2-U

National Research Council (2015a). *Climate intervention: Carbon dioxide removal and reliable sequestration*. Washington, DC: The National Academies Press. https://doi.org/10.17226/18805

National Research Council (2015b). *Climate intervention: Reflecting sunlight to cool Earth*. Washington, DC. https://doi.org/10.17226/18988

Niemeier, U., Schmidt, H., Alterskjær, K., & Kristjansson, J. E. (2013). Solar irradiance reduction via climate engineering: Impact of different techniques on the energy balance and the hydrological cycle. *Journal of Geophysical Research: Atmospheres*, *118*, 11,905–11,917. https://doi.org/10.1002/2013JD020445

Pörtner, H.-O., Karl, D. M., Boyd, P. W., Cheung, W., Lluch-Cota, S. E., Nojiri, Y., et al. (2014). Ocean systems, *Climate change 2014: Impacts, adaptation, and vulnerability. Part A: Global and sectoral aspects. Contribution of Working Group II to the Fifth Assessment Report of the Intergovernmental Panel on Climate Change* (pp. 411–484). New York: Cambridge University Press.

Quintero, I., & Wiens, J. J. (2013). Rates of projected climate change dramatically exceed past rates of climatic niche evolution among vertebrate species. *Ecology Letters*, *16*(8), 1095–1103. https://doi.org/10.1111/ele.12144

Ramaswamy, V., Boucher, O., Haigh, J., Hauglustaine, D., Haywood, J., Myhre, G., et al. (2001). Radiative forcing of climate change, *Climate change 2001: The scientific basis. Contribution of working group I to the Third Assessment Report of the Intergovernmental Panel on Climate Change* (pp. 349–416). New York.

Renforth, P., & Henderson, G. (2017). Assessing ocean alkalinity for carbon sequestration. *Reviews of Geophysics*, *55*(3), 636–674. https://doi.org/10.1002/2016RG000533

Royal Society (2009). *Geoengineering the Climate: Science, Governance and Uncertainty (RS policy document 10/09)*. London, England: The Royal Society.

Schmidt, H., Alterskjær, K., Bou Karam, D., Boucher, O., Jones, A., & Kristjánsson, J. E. (2012). Solar irradiance reduction to counteract radiative forcing from a quadrupling of $CO_2$: Climate responses simulated by four Earth system models. *Earth System Dynamics*, *3*(1), 63–78. https://doi.org/10.5194/esd-3-63-2012

Serreze, M. C., & Barry, R. G. (2011). Processes and impacts of Arctic amplification: A research synthesis. *Global and Planetary Change*, *77*(1), 85–96. https://doi.org/10.1016/j.gloplacha.2011.03.004

Sonntag, S., Ferrer González, M., Ilyina, T., Kracher, D., Nabel, J. E. M. S., Niemeier, U., et al. (2018). Quantifying and comparing effects of climate engineering methods on the Earth system. *Earth's Future*, *6*, 149–168. https://doi.org/10.1002/2017EF000620

Stier, P., Feichter, J., Kinne, S., Kloster, S., Vignati, E., Wilson, J., et al. (2005). The aerosol-climate model ECHAM5-HAM. *Atmospheric Chemistry and Physics*, *5*(4), 1125–1156. https://doi.org/10.5194/acp-5-1125-2005

Tjiputra, J. F., Grini, A., & Lee, H. (2016). Impact of idealized future stratospheric aerosol injection on the large-scale ocean and land carbon cycles. *Journal of Geophysical Research: Biogeosciences*, *121*, 2–27. https://doi.org/10.1002/2015JG003045, 2015JG003045

van Vuuren, D., Edmonds, J., Kainuma, M., Riahi, K., Thomson, A., Hibbard, K., et al. (2011). The Representative Concentration Pathways: An overview. *Climatic Change*, *109*(1-2), 5–31. https://doi.org/10.1007/s10584-011-0148-z

Wolf-Gladrow, D. A., Zeebe, R. E., Klaas, C., Körtzinger, A., & Dickson, A. G. (2007). Total alkalinity: The explicit conservative expression and its application to biogeochemical processes. *Marine Chemistry*, *106*(1-2), 287–300. https://doi.org/10.1016/j.marchem.2007.01.006

Wurts, W. A., & Durborow, R. M. (1992). Interactions of pH, carbon dioxide, alkalinity in fish ponds. https://doi.org/10.1.1.212.840